SCIENCE CHINA
Earth Sciences

• RESEARCH PAPER •

December 2012 Vol.55 No.12: 2068–2083
doi: 10.1007/s11430-012-4524-y

On temporal-spatial distribution of backscatter coefficients over China determined by TOPEX/Poseidon mission

GUO JinYun[1,2,3*], YANG Lei[1], LIU Xin[1,2], HWANG CheinWay[4] & YANG Hong[1]

[1] *College of Geodesy and Geomatics, Shandong University of Science and Technology, Qingdao 266590, China;*
[2] *Key Laboratory of Surveying and Mapping Technology on Island and Reef of NASMG, Qingdao 266590, China;*
[3] *National Astronomical Observatories, Chinese Academy of Sciences, Beijing 100012, China;*
[4] *Department of Civil Engineering, Chiao Tung University, Hsinchu 300, Taiwan, China*

Received February 3, 2012; accepted September 8, 2012; published online September 27, 2012

This paper deals with the backscatter coefficients known as sigma0 at Ku band and C band based on the GDR-M (Merged Geophysical Data Record) of TOPEX/Poseidon (T/P) through Jan. 1993 to Dec. 2004 over land surface of China. After smoothing and interpolating the backscatter coefficients for both bands, we achieve the 5′×5′ grid data and the time series of backscatter coefficients in 12 years. The spatial distribution of sigma0 over typical areas (wetland, desert, mountainous area, agriculture base, etc.) of Chinese territory is analyzed and discussed. The fast Fourier transformation (FFT) is used to detect the cycles of seasonal variations of sigma0 time series and gives that the annual period is the major cycle. Meanwhile a semi-annual period is also found in some places. We use the least squares method on both periods and find that the amplitude of annual period is obviously greater than that of semi-annual period. The relationship among the anomalousness of time series, variations of environment and climate change, and the serious natural calamity (flood, drought) is also discussed. Data of topography slope extracted from SRTM are used to do correlation analysis with the backscatter coefficients in parts of China to quantify the impact of slope on backscatter coefficients in Ku and C bands, and the results show that they all have a negative correlation but the magnitudes are different in different places with different coverages. Such as the area of Liaoning and Jilin has the maximum correlation –0.56, the Taklimakan Desert has the minimum correlation –0.11, and the other places commonly have correlations in (–0.3, –0.5).

backscatter coefficient, satellite altimetry, TOPEX/Poseidon, land surface, SRTM

Citation: Guo J Y, Yang L, Liu X, et al. On temporal-spatial distribution of backscatter coefficients over China determined by TOPEX/Poseidon mission. Sci China Earth Sci, 2012, 55: 2068–2083, doi: 10.1007/s11430-012-4524-y

Satellite radar altimeters are designed primarily to measure the topography of ocean surface by the active radar [1]. The distance from the satellite to a reflecting target surface can be determined by measuring the satellite-to-surface round-trip time of a radar pulse [2]. Looking at the returned waveform, we can also measure the wave height and the wind speed over oceans, the backscatter coefficient and the surface roughness for most surfaces off which the radar signals are reflected [3]. The satellite altimeter optimized for the ocean detection continues to transmit radar pulses and receive echoed signals while flying over lands. We all know that the land surfaces are more complex and not spatially homogeneous. The inhomogeneous land surface makes it more difficult to precisely interpret waveforms over lands and to retrack them than over oceans [4–7]. Satellite altimetric application over lands, such as the detection of the Antarctic ice sheet height and snow property, the monitoring of lake level change and desert height variation, and the improvement of digital elevation model globally, is one

*Corresponding author (email: jinyunguo1@126.com)

important topic of satellite altimetry [8–16].

The backscatter coefficient known as sigma0 is an important measurement in the radar altimetry over lands. The backscatter coefficient yields interesting land information since it depends on the characteristics of the reflected surface, for example, covered by snow, vegetation, flooded areas, surface roughness, etc. [3, 17]. Big deserts and ice-covered surfaces with small regional slopes are studied mainly by the satellite altimetry technique [5]. The height change of Antarctic ice sheet is sensitive to the sea level variation, and the snow penetration property over ice sheet can be studied with the dual-frequency radar satellite altimeter [16, 18]. The sigma0 over deserts is very stable because the desert area has little rain per year and the vegetation is rare. The desert is a better place for calibration of satellite radar altimeter [19, 20]. It is also an ideal place to collect measurements in situ for a deep understanding of the effect of surface roughness, slope, soil moisture, and presence of vegetation because the desert is simpler than other land types [11]. In situ measurements over deserts are also very useful for improving the backscatter model and calibration of radar altimetric data.

We can recognize the main land types from the global or regional backscatter image of TOPEX/Poseidon (T/P) dual-frequency radar altimeter, such as mountain, desert, tropical forest, wetland, wet and dry savanna, and ice sheet [12, 21–23]. The sigma0 has the related seasonal variation because of the seasonal changes of land coverage, and then the backscatter coefficients determined with the satellite altimeter can be used to investigate the land surface variations and environment changes globally or regionally. Improving the precision of the backscatter coefficients by retracking waveform is also a key topic of land altimetric applications as the retracking methods are mostly designed for ocean or ice sheet and only one elementary expert retracking system was ever designed for land areas [22, 24]. Because of the unsolved conflict of spatial and temporal resolutions, it is important to merge data of different altimeter missions to achieve better spatial and temporal resolution. The potential to detect backscatter coefficients over land surfaces with multi altimeters was investigated and merging multi-altimeter data can improve the poor spatial and temporal resolution of single altimeter measurements [23].

Although the land altimetry has achieved some results, the data used in pre-researches have small time span and the researched areas were often at global scale or focused on local areas such as deserts and ice sheets. There still lacks the temporal-spatial analysis of backscatter coefficients from radar satellite altimetry over the main land of China. This paper will show the temporal-spatial distribution of backscatter coefficients over China determined with the dual-frequency T/P altimeter, that is, Ku and C bands, in 12 years from Jan., 1993 to Dec., 2004. The fast Fourier transformation (FFT) and the least squares method [25], respectively, are used to calculate the cycles and amplitudes of the sigma0 time series over 12 years, and then the spatial and temporal distribution of sigma0 over China is analyzed. We also discuss the sigma0 time series over some significant areas such as wetlands, deserts and plains according to the characteristics of land physical geography. The anomalous signals in the time series are also discussed to explore if there exist relationships between sigma0 and some strong natural disasters happened in 1993–2004 such as drought and flood. At last we determine the effect of slope on sigma0 by doing correlation analysis between the sigma0 and the slope derived from the shuttle radar topography mission (SRTM) (http://www2.jpl.nasa.gov/srtm/).

1 Data and methods

T/P is a jointed mission between the National Aeronautics and Space Administration, USA (NASA) and the Centre National d'Etudes Spatiales, France (CNES) that was launched on Aug. 10, 1992 with the main objective of observing and understanding the ocean circulation [26]. An inclination of 66° was selected so as to cover most of the world's oceans (~90%). A repeated period of 9.916 d was chosen as the best compromise between spatial and temporal resolutions [3]. It carried two radar altimeters, that is, the TOPEX which operates on two microwave bands at 13.6 and 5.3 GHz to determine the electron content in the atmosphere, and the Poseidon which uses one single Ku band. Although the use of dual frequencies is primarily for correction of ionospheric delay, it is useful for the land altimetry because microwave pulses at different frequencies have different capacities of penetration for land coverages. The two altimeters used one same antenna and the TOPEX occupied it nearly 90% of total working times [3, 27, 28]. On Sept. 15, 2002, T/P assumed a new orbit midway between its original ground tracks. The former T/P ground tracks are now overflown by Jason-1.

Backscatter coefficients can be extracted from the geophysical data records (GDRs) or derived from the returned waveforms as a kind of altimeter measurements [29]. The simplified equation of the radar altimeter sigma0 can be deduced from the radar equation [2], given

$$\sigma_0 = \frac{P_r 64\pi^2 \left(1+h/R_{\mathrm{e}}\right)}{P_{\mathrm{t}} G^2 \lambda^2 c\tau} h^3 L_{\mathrm{att}} L_{\mathrm{atm}} L_T , \quad (1)$$

where G is the boresight antenna gain, P_r the received power, h the satellite orbit altitude, R_{e} the earth radius, P_t the transmitted power of antenna edge, λ the radar wavelength, c the speed of light, τ the pulse width, L_{att} the altitude angle attenuation, L_{atm} the atmospheric attenuation, and L_T the attenuation related with temperature.

The backscatter coefficient results from two contributions: a surface echo scattered by an interface between two dissimilar mediae and a volume echo scattered by particles

inside a medium. These two contributions depend on the land target characteristics, the radar footprint (partially depending on the surface roughness and slope), and the quantity of surface scatters within the footprint. Some returned signals are only due to the surface echo controlled by the dielectric constant and the surface roughness of the target over inland water surface, inundated soils, melting snow, and several solid bare soils. Some returned signals are due to reflecting surfaces located under volumetric scatterers over sparse forests, inundated forests, and dry snow-covered areas. And some returned signals are due to reflecting surfaces situated above volumetric scatters that are expected for dry or arid areas, wet snow-covered areas, and some vegetated areas [12].

Figure 1 shows the ground tracks of T/P over China. Sigma0s over China are extracted from 12 years of GDRs of T/P. GDR-Ms are altimeter products in AVISO/Altimetry CD ROMs containing merged T/P GDRs version C. A GDR-M consists of ten-day repeated cycles of data. It is organized as a cycle header file and a maximum of 254 pass-files. A pass-file contains altimeter data from a satellite pass (half a revolution). Elementary records in a pass-file are in 1 Hz, but may be discontinuous if measurements are not available. Firstly, we extract sigma0s for Ku and C bands over China land area and the neighboring land zone (17°–54°N, 73°–135°E) from T/P GDRs based on the data rules of AVISO [27]. Because data over lands are asymmetrical and less than ocean data, we estimate the monthly mean sigma0 values through continuous three cycles and get 12 files of average values along ground tracks each year. Then we smooth all the along track data and interpolate them to 5′×5′ regular grid data using the adjustable tension continuous curvature surface gridding algorithm [30, 31]. So each grid point has a time series of 12 years. After that, we use FFT and the least squares method to analyze the time series of each grid point to estimate the temporal changes, amplitudes of both cycles and trend values, which are used to discuss the temporal and spatial distribution of backscatter coefficients over China.

2 Spatial distributions of backscatter coefficients

Figure 2 shows the mean values of T/P backscatter coefficients for Ku and C bands, and the differences of backscatter coefficients for these two bands over China and adjacent land areas in 12 years.

For Ku band, we can find that the sigma0 values commonly range from 0 to 30 db and the mean sigma0 of all grid points is 11.32 db. For C band, the sigma0 values range commonly from 5 to 30 db and the mean value is 15.40 db. Some areas have a significantly higher backscatter values than 30 db such as big river basins and wetlands because the effect of specular reflection of water surface and the soil moisture is much higher, which affects the dielectric constants. For example, in the Yangtze River Basin, the mean value is 27.31 db and the maximum value is 40.16 db for Ku band and the two values are 30.39 and 43.30 db for C band respectively. The maximum values of backscatter coefficients over the study area are 43.30 and 47.44 db respectively for Ku and C bands located at nearly the same place over the Ganges downstream.

Obviously, backscatter coefficients are commonly higher at C band than these at Ku band, and it also shows some similar characteristics of distribution for Ku and C bands. Over mountainous areas, the sigma0 values are generally low for both bands, which may be directly due to the complex land surface and the presence of topographic slopes, as the altimeter antenna convoluted with the angle of incidence (0.6° in Ku band and 2° in C band) reduces the returned power of the altimeter echo [12]. Some significant mountains are easily distinguished in Figure 2 for both bands due to lower values of backscatter coefficients, such as the Himalayas, the Da Higgan Mountains, the Taihang Mountains, the Tianshan Mountains, and the Altay Mountains. But these mountains are slightly clearer at C band than at Ku band because C band is less sensitive to small-scale roughness than Ku band so that the impact of topography slope is highlighted.

It shows high sigma0 values for both bands over some flat plains or large river basins. Especially over the estuaries of the Yangtze River and the Yellow River the sigma0 values are especially high, and the C band values exceed 30 db and the Ku band values exceed 25 db. The Tarim River is very clear in Figure 2 and the sigma0 values here are high because the existing water surface reflects altimeter pulses strongly. In addition to river basins, some great plains such as the Northeast China Plain, the Northern China Plain, and the Middle-lower Yangtze Plain also have high sigma0 values mainly due to the less fluctuating land surface, higher soil humidity, and the presence of vegetations. We can also

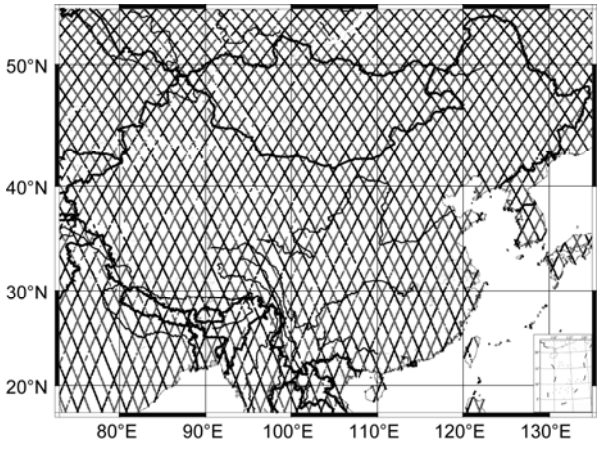

Figure 1 The ground tracks of T/P in China. The red line represents track after orbit changing in 2002 and the black line represents track before orbit changing.

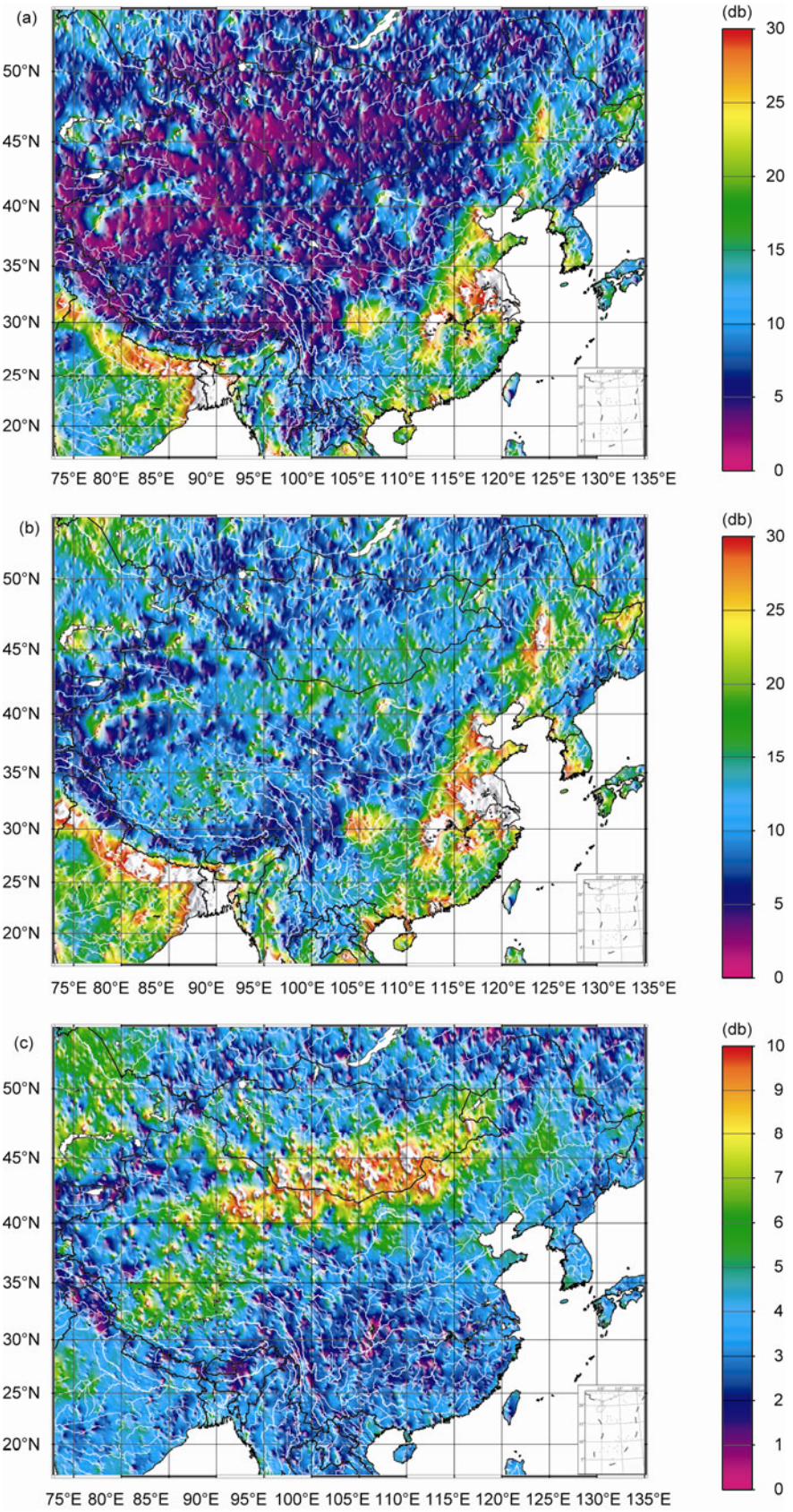

Figure 2 The distribution of backscatter coefficient over studied areas based on T/P altimeters during 1993–2004. (a) The mean value of Ku band; (b) the mean value of C band; (c) the mean difference of both bands.

find that the Ganges River Basin located at the south of China has significantly high sigma0 values as a sharp contrast with the Himalayas. On one hand, the higher sigma0 value is due to the flat topography with the small slope and roughness. On the other hand, it is due to the presence of the Ganges water area, because even a very small area of water can be the domination of the sigma0 for its specular reflection of radar pulse [12]. Over the big river basins, there are many lakes and tributaries of rivers, so the water storage is abundant. In addition, the soil moisture that contributes to the dielectric constant also has high values in these areas, which has a positive effect on the sigma0 values.

Figure 2 also shows the spatial distribution of sigma0 difference for C and Ku bands. For different frequencies of radar pulse, the penetrating capacities to soil and land vegetation are not the same so that the sigma0 presents respective values with two different bands over the land surface. The sigma0 differences are commonly between 0–10 db, which indicates that the backscatter coefficient is higher at C band than at Ku band as a whole.

The mean sigma0 difference for C and Ku bands is 4.08 db and the standard deviation is 1.72 db in the study area. The big differences lie on the northern Tibetan Plateau and in the Junggar Basin, the Tarim Basin, and the Shunha Gobi in Xinjiang, especially deserts or Gobi areas around the Inner Mongolia (such as Badan Jaran, The Central Gobi, the Mu Us Desert), because soil humidity and the percentage of vegetation coverage over these areas are low. The differences are also slightly higher in Northeast China and Kazakhstan than those over Southern China for the high soil humidity resulted from the plentiful rainfall over South China.

Figure 3 shows the average sigma0 values of 12 months in 1 year and monthly value is calculated from 12 years' (1993–2004) sigma0s, indicating that the monthly change is significant in some places for both bands. For example, over parts of the Tibetan Plateau, the sigma0 is low during winter (Dec., Jan., and Feb.) and high during summer (Jul., Aug., and Sept.), which is probably due to the seasonal changes of land surface and coverage, such as the seasonal growth of vegetation, the thaw and freeze of frozen soil, and the seasonal precipitation.

For the radar satellite altimeter, backscatter coefficients depend on the condition of land surface covered by the vegetation, snow and/or flood [3]. From the analysis in this section, it can be found that backscatter coefficients are high over the marshes, river basins, rainy areas, and flat areas, whereas low values can be found over the arid places and mountains. Actually, the special distribution of sigma0 is affected mainly by the topography and the dielectric constant of land surface. The backscattering power is high over flat surfaces, which lead to high sigma0 but small over roughness surfaces lead to low sigma0. The dielectric constant closely related to backscatter coefficients can change under the effect of ground water contents, and so sigma0 is high over big river basins, rainy areas of Southern China, and wetlands. The spatial distributions of backscatter coefficients for Ku and C bands are in accordance with the researches on the global scale in [12].

3 Analysis of the time evolution of backscatter coefficients

As discussed in the above section, the backscatter coefficient is related to the property of land surface. Since vegetations, rivers, snow covers, moisture, and frozen soils in some places have significant seasonal variations and the seasonal precipitation, the land coverage, and soil property in most places of China change seasonally, the backscatter coefficient changes seasonally. And we have done some preliminary researches on the evolution of sigma0 in section 3, based on which we make a further analysis of time series of sigma0 to study the seasonal signals of periodic variations. Then some special cases combining with characteristics of China's nature topography are shown.

3.1 FFT analysis of time series of sigma0 in 12 years

Figure 4(a) shows temporal variations of mean sigma0s for Ku and C bands, as well as their differences, using 12 years' original data along ground passes over the study areas (17°–54°N, 73°–135°E). It is clear that the time series in two bands have significantly similar sinusoidal signals, indicating that seasonal change of backscatter coefficients really exits and is commonly synchronous for these two bands. The mean sigma0s from the time series for Ku and C bands are 13.24 and 15.46 db, respectively. The correlation coefficient of backscatter coefficients between Ku and C bands is 0.96, a strong positive correlation, indicating that backscatter coefficients at these two bands have the same trend up or down as a whole. The mean sigma0 difference for C and Ku is 2.22 db, and the time series of differences also have seasonal variations but the amplitude is smaller than those for C and/or Ku band. For the widely studied area with the diverse land surfaces, the backscatter coefficients are not the same from one place to another. In addition, the evolution of backscatter coefficient has no synchronization in the time field, and so Figure 4(a) only shows the common trend of backscatter coefficients and masks variations over some areas. Therefore, the temporal variations over the regional area should be independently analyzed.

In order to find main cycles of time series, the FFT method is used and the results are shown in Figure 4(b) for Ku and C bands, respectively. The power spectra for both bands are nearly the same and the main period is annual. And the semi-annual period possibly exiting in some areas does not clearly appear because the less synchronization for backscatter coefficients over land surfaces in the

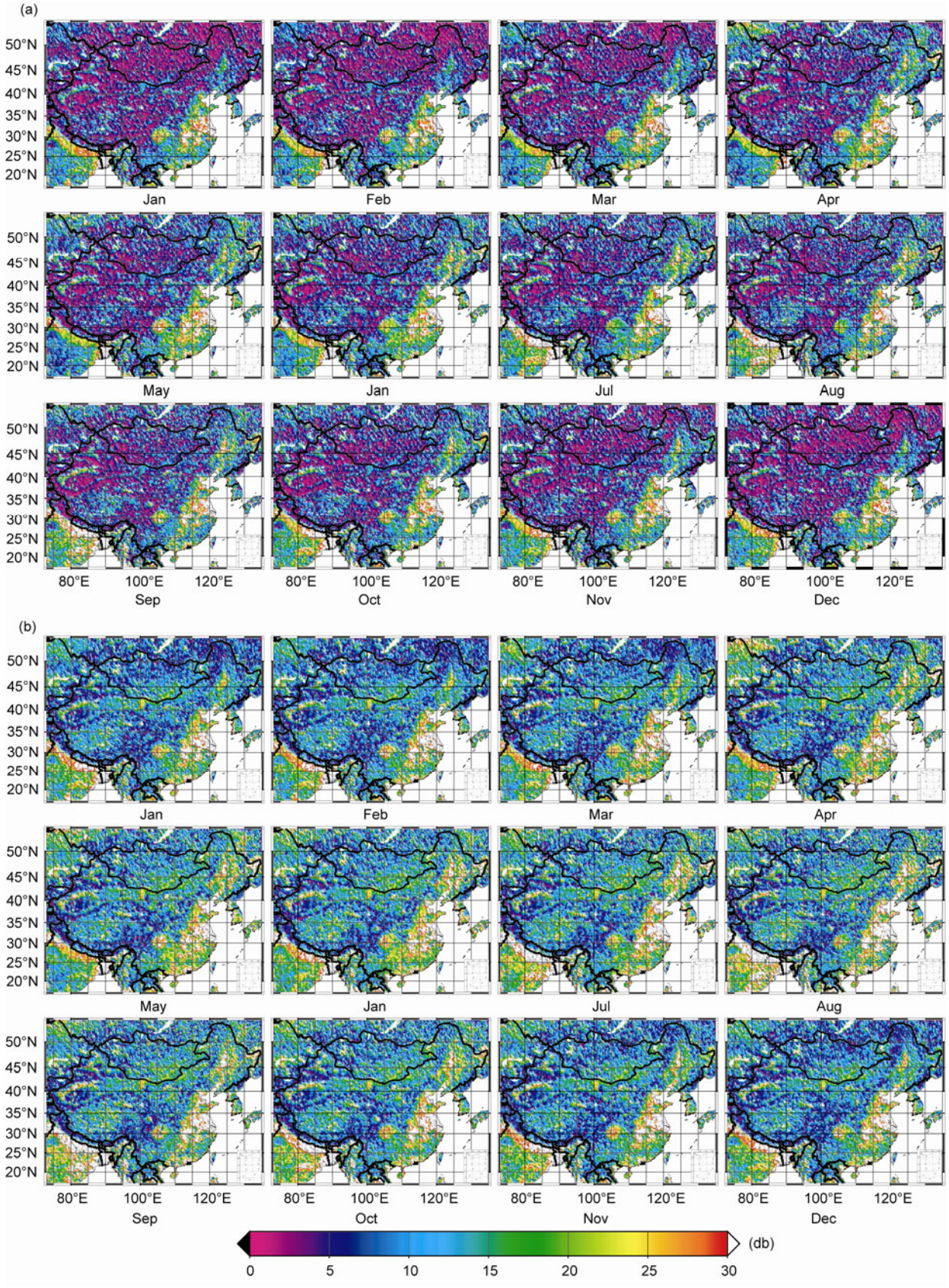

Figure 3 The monthly evolution of backscatter coefficients averaged from 12 years (1993–2004) over studied area. (a) Ku band; (b) C band.

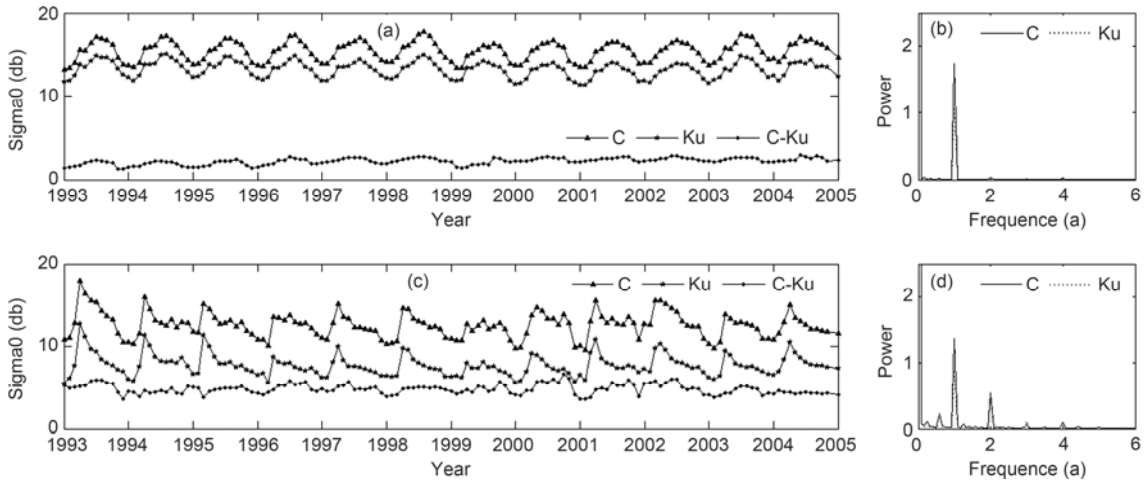

Figure 4 (a) Time series of backscatter coefficients averaged of ground pass data over the studied area in Ku, C and sigma0 difference; (b) the spectrum analysis for Ku and C bands; (c) the time series for Ku, C and sigma0 difference; (d) the spectrum analysis for Ku band over Kazakhstan areas (47°–51°N, 73°–79°E).

semi-annual period over China. We select the regional area of Kazakhstan (47°–51°N, 73°–79°E) to confirm the semi-annual period, and the result shown in Figure 4(c) and (d) indicates that the semi-annual period exists as a minor cycle. There may also exist other periods but with the poor power, so we only consider the annual and semi-annual periods and calculate the periodic parameters of time series by the least squares method in order to get an optimum fitting result over the whole area.

3.2 Periodic analysis with the least squares method

The least squares method can be used to estimate the amplitudes, trends, and phases of time series on each grid point by fitting the polynomial equations with unknown periodic parameters [25]. Amplitude is the focused parameter in our study, which reflects the magnitude of sigma0 variations. As mentioned in the former sections, the seasonal variation of backscatter coefficients is related to land surface changes, such as seasonal changes of precipitation, vegetations, soil moistures, and snow covers. It is useful to detect variations and the magnitude of land coverage or soil properties by calculating the amplitude of the sigma0 time series. Trends are valuable in the research of environment and climate changes in some fragile ecosystems like grasslands and wetlands, because trends coming from a long history dataset can predict whether the grasslands or wetlands will expand or shrink. The initial phase represents the time point when the change happens and can be used to study differences of the environment and climate over different places, especially in China, since the territory is extremely vast and there coexists multiple climates causing the growing of vegetations out of sync.

Figure 5 shows the amplitude distributions of annual and semi-annual periods of sigma0 time series for C and Ku bands, and Table 1 lists the statistics of the amplitude and correlation coefficients for C and Ku bands, from which we can sum up as follows.

(1) Spatial distributions of amplitudes for Ku and C bands are relatively consistent, and so is the magnitude for each period. The correlation coefficients of amplitudes for two bands in annual and semi-annual periods are 0.96 and 0.93 respectively, indicating that although magnitudes of backscatter coefficients are different, the amplitudes are nearly identical.

(2) In China the most significant area for high amplitudes of both period variations is in the Northeast Plain (43°–49°N, 121°–133°E) where the mean value of amplitudes of each grid points at Ku band is 4.71 db, and the highest point (47.3°N, 132.9°E) is located at the wetland of the Three River Plain in Heilongjiang Province. For annual variations at two bands, the amplitudes at the origin of three-river origin areas in Qinghai Province, parts of South China, most of Southeast Asia, and parts of Central Asia over studied areas are remarkable, too. For the semi-annual variations at two bands, the Sichuan Basin, a developed agriculture base, is significant for Ku band. In addition, there exist many small areas with high amplitudes, such as the Zoige Wetland, the Hetao Plain, the Tarim River Basin, and desert oasis in the Taklimakan Desert.

(3) Some regions in China have the low amplitudes, implying that seasonal variations of backscatter coefficients are not notable. Especially over the broad areas in North-

Table 1 Statistics of amplitudes of backscatter coefficients in the study area

Period	Band	Mean amplitude (db)	Correlation coefficient
Annual	Ku	1.64	0.96
	C	1.63	
Semi-annual	Ku	0.80	0.93
	C	0.78	

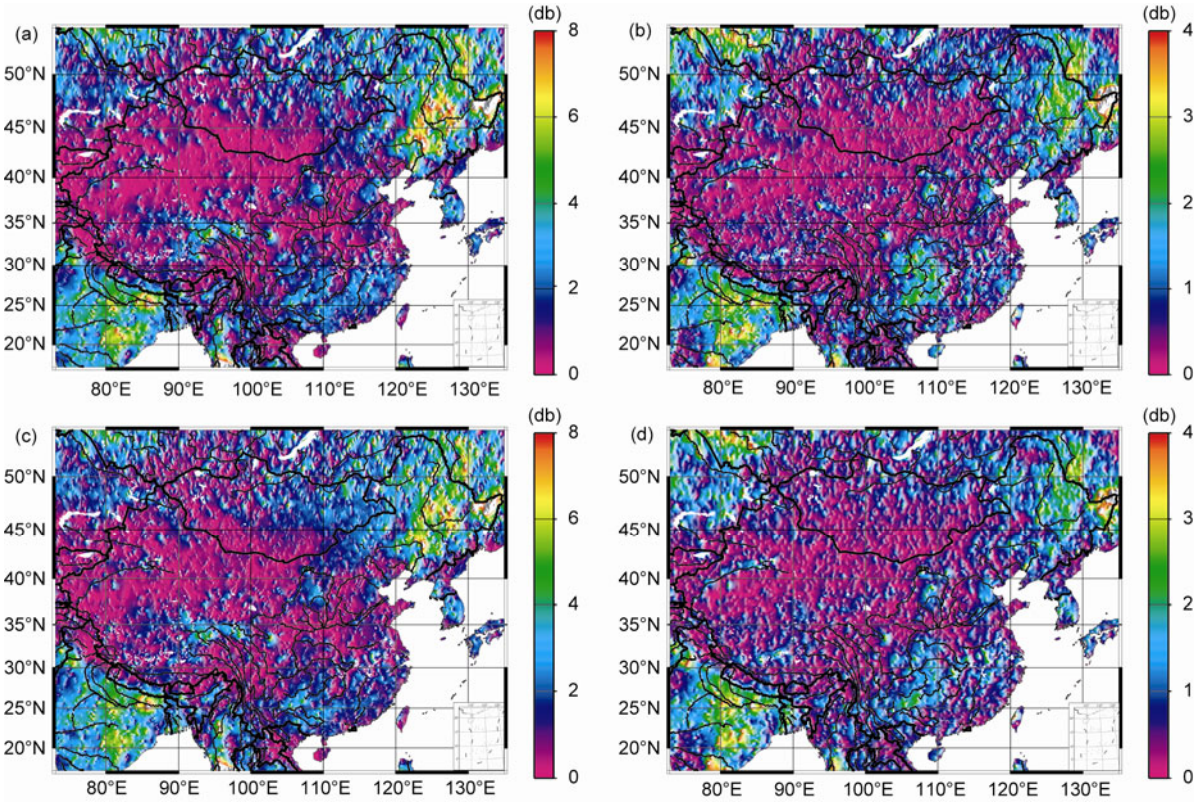

Figure 5 Amplitudes for annual and semi-annual periods. (a) The annual period of Ku; (b) the semi-annual period of Ku; (c) the annual period of C; (d) the semi-annual period of C.

west China, the amplitudes are close to 0 db due to the widely existing of Gobi or desert land types with little vegetation and the arid climate with little rainfall.

(4) Amplitudes of annual variations are about twice that in the semi-annual variations for two bands, which is corresponding to the FFT results that annual period is the main circle and semi-annual is the minor one. In general, this is also consistent with the vegetative characteristics in China.

(5) A distribution gradient of amplitudes for two bands and two periods along the Himalayas is significant with high values over southern areas of the Himalayas and low at South Tibet. For the Himalayas and most parts of Tibet, the land coverage and soil humidity change slightly compared with southern areas of the Himalayas. Particularly in Bangladesh and India, the volume of seasonal rainfall (Jun. to Oct.) accounts for 80% of the whole year because of the monsoon climate.

(6) Amplitudes at the three-river origin area in Qinghai are conspicuous for annual variations but inconspicuous for semi-annual variations. This is mainly due to the growth characteristics of psychrophyte and the special climate on the Tibetan Plateau.

(7) Amplitudes in the Sichuan Basin and parts of South China are more conspicuous for semi-annual variations than annual variations, which is related to local agriculture and seasonal water content of soil.

Table 1 gives the statistics of amplitudes of simga0 in our study areas, proving that the mean amplitudes of the two bands for both cycles have little difference and the correlation coefficients of spatial distributions for two bands are very high. We can conclude that although sigma0s in C band are higher than those in Ku, the magnitudes and distributions of seasonal variations of sigma0s in two bands are nearly the same.

3.3 Analysis of regional cases

In consideration of characteristics of China's physical geography and spatial-temporal distributions of backscatter coefficients, we select five sites as the specially studied cases, that is, the Northeast Plain, the Hetao Plain, Zoige, the Sichuan Basin, and the Taklimakan Desert (Figure 2).

3.3.1 Northeast China Plain

The Northeast Plain, located among the Da Hinggan Mountains, the Xiao Hinggan Mountains, and the Changbai Mountains, is the biggest plain in China with an area of 350000 km^2. It contains three parts: the Three-river Plain due to influence of the Heilong River, the Songhua River, and the Wusuli River in Northeast China; the Songnen Plain in the middle is named by the Songhua River and Nenjiang River; and the Liaohe Plain is located in the south, named

after the Liaohe River. This is the biggest distribution area of marsh, mainly including freshwater bogs and lakes, as well as rivers and artificial wetlands. Now some agricultural bases are built, such as the Beidahuang in the past, and meanwhile the ecological balance is broken in some way and weather conditions are exacerbated that cause the decrease of rare animals and plants. It is meaningful to detect the changes of wetlands by studying the variation of the land surface coverage using radar satellite altimeters from space.

Figure 5 indicates that the Northeast Plain is the biggest regional area with the remarkable amplitudes of sigma0 in China. The amplitudes of annual variations range from 4 to 8 db and the mean value of all grid points is 4.71 db at Ku bands. Especially over the Three-river Plain, amplitudes of annual variations exceed 8 db in some places and those of semi-annual variations exceed 4 db. Amplitudes at C bands mainly agree with those for Ku bands, so we mainly discuss the Ku band unless otherwise specified.

Figure 6(a) and (b) shows time series of mean backscatter coefficient, respectively, averaged in month and year using the original pass values over the Northeast Plain for Ku, C bands and their difference. Figure 6(d) is a statistical histogram that presents the maximum changes of backscatter coefficients calculated by subtracting the maximum value with the minimum value of each year. Values in Figure 6(c) reflect the absolute variations of land surface coverage in one year, which is related with the amount of seasonal vegetations and whether rainfalls are concentrated.

Figure 6(a) shows significant seasonal variations of sigma0 for Ku and C bands, characteristics of sinusoidal time series for two bands, and relative stability of differences for both bands in 12 years. The peaks of time series for two bands are all present in the summer of 1998 with values of 23.48 and 20.03 db at C and Ku bands, respectively. Figure 6(a) and (c) also shows that the year 1998 is an abnormal year while an extraordinary flood happened over Northeast and South China. And the flood magnified the soil humidity and specular reflection and was the main contribution to the abnormal sigma0. The troughs of low sigma0 values appeared in the spring of 1993 and 2001 from Figure 6(a), which were 8.06 db at Ku band and 11.59 db at C band in 2001, and the trough of Figure 6(c) is also in 2001 with low values of 12.83 db for Ku band and 11.92 db for C band. We know that a great drought affected many parts of China including the Northeast Plain in 2001 that caused rivers or lakes out of water and mud cracking. In addition, the mean value of sigma0 in the time series for Ku band is 14.38 db and that for C band is 17.42 db, and the difference values for both C and Ku bands were steadily at 3 db with slight variations. The minimum values in Figure 6(c) are present in 2004, 7.10 db for Ku band and 7.50 db for C band, and the maximum values in Figure 6(d) (11.15 db for C band and 10.66 db for Ku band) are shown in 1993, probably resulting from the unsteadiness of initial run of T/P altimeters and the climate of that year (http://www.people.com.cn/GB/huanbao/259/index.html).

The high amplitudes over the Northeast Plain significantly reflect the seasonal variations of land reflecting media. The reasons for this may be as follows.

Crops are widely planted in the agricultural bases because of the rich soil and water there, which have significant seasonal variations.

Soil humidity and water content of rivers, lakes, and wetlands vary seasonally. There are several big rivers and the widest marsh areas, such as the Heilong River, the Songhua River, the Nen River, the Wusuli River and Sanjiang wetlands, which contain abundant water resources. And the dielectric constant related to the water content is affected by the seasonal precipitation concentrated in the summer and frozen phenomenon of river and soil in winter. The changes of dielectric constant also cause variations of backscatter coefficients.

The snow cover in winter also contributes to the seasonal

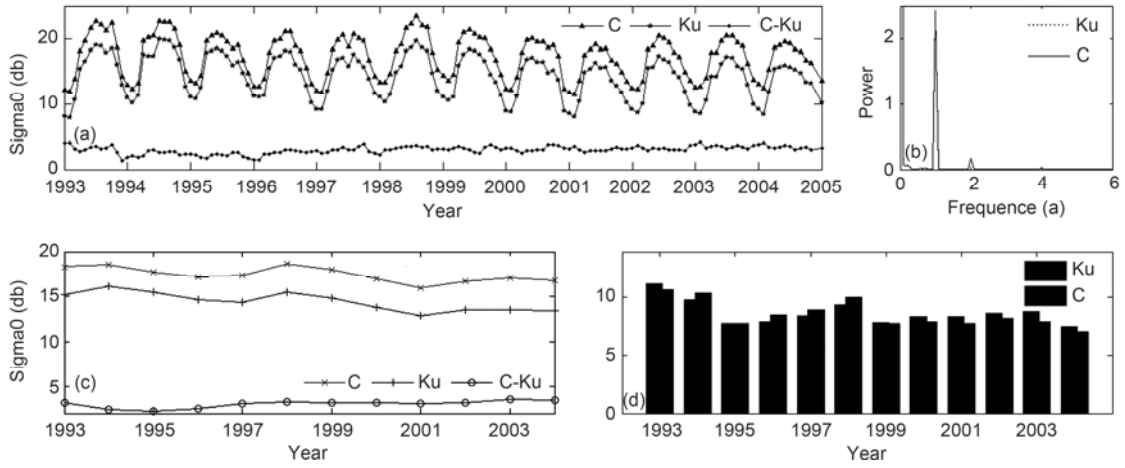

Figure 6 Time series of backscatter over the Northeast Plain. (a) Monthly mean value; (b) the spetrum analysis for backscatters in Ku and C bands; (c) yearly mean value for Ku and C bands, as well as difference values of two bands; (d) the maximum values of variations each year for Ku and C bands.

change of sigma0.

For the diverse soil types and vegetations in the wide plain, reasons for different places may be different and need further research and analysis.

3.3.2 Hetao Plain

As an alluvial plain, the Hetao Plain is located in the hoof-like corner of the Yellow River, which is the biggest irrigation agriculture area in Asia with the flat land and numerous graffes. The precipitation is rare and the evaporation capacity is significant in the Hetao Plain, but here has abundant water content for the pass of the Yellow River [32]. Figure 7(a) indicates that there exists a great difference of environment between Hetao (the green part) and surrounding areas (mainly deserts and gobi lands with arid soils and few plants). So this is a proper site for studying the difference of backscatter coefficients over two distinctive land types.

Shown in Figures 5 and 7(b), the Hetao Plain is easy to distinguish for its high amplitudes of annual variations ranging from 4 to 7 db at Ku band, and the maximum value 6.94 db appears at the central position. Amplitudes of semi-annual mainly lie in 2–4 db, and the maximum value also appears at the center.

Figure 7(b) shows that there is a cross-point in the Hetao Plain before shifting orbit of T/P, and the passes moved to deserts around Hetao after shifting orbit that resulted in a large leap of time series in 2002 in Figure 7(c). The sigma0 values decrease greatly at two bands, and so are the differences of C and Ku bands after shifting orbit. Meanwhile, Figure 7(e) shows that the absolute variations of backscatter coefficients decreased sharply to small values, which is consistent with the change of ground pass from farmlands to the arid land. The sigma0s before 2002 at two bands show evident seasonal signals, and the amplitudes of annual and semi-annual variations for Ku band are 3.18 and 2.24 db, respectively. The mean difference value is 1.51 db and the crest of difference time series generally appears in January when the Yellow River is poor and is the most arid period of the year. Figure 7(c) also reveals another important information that two or three peaks coexist every year, which is probably associated with local precipitations, the flood season of Yellow River, and the growth of plants. The first peak presents in March when the vegetations revive to green and farmers water their cornfields, which causes the increase of soil humidity. The second peak presents from

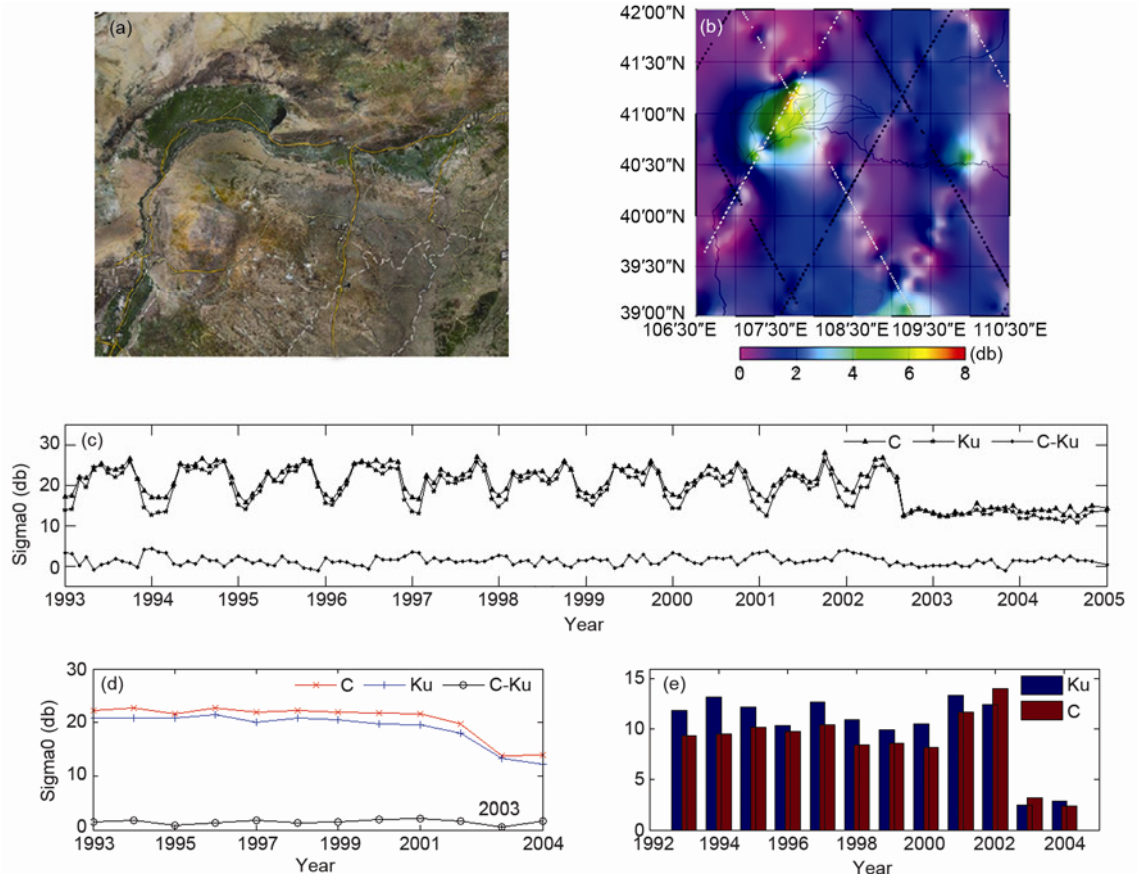

Figure 7 (a) The satellite image of Hetao area; (b) the distribution of amplitudes of annual variations at Ku band over the Hetao Plain and ground passes of T/P of which the white line is pre-orbit and the black is post-orbit; (c) the time series of monthly mean backscatter over Hetao Plain; (d) the yearly mean value, at Ku and C bands, as well as difference values of two bands; (e) the maximum of annual variations each year for Ku and C bands over the Hetao Plain.

May to June for the leaf area of plants reaches the top and then the backscatter coefficient decreases as the reaping of wheat. The third peak presents in October, which may be caused by the autumn flood of the Yellow River. From Figure 7(d) and (e), the normal backscatter coefficients in 1998 indicate that this area is not affected by the extraordinary flood happened in 1998, and this is in accordance with the hydrology situation of the Yellow River in 1998. And in 2001, a drought happened in most areas of China with very few precipitations besides some areas including the Hetao Plain (http://www.weather.com.cn/zt/kpzt/1244064.shtml), which is consistent with Figure 7(e) and (c).

Some other factors affected the seasonal variations of backscatter coefficients over the Hetao Plain may be as follows.

(1) The Hetao Plain is a developed agricultural area and the growth of plants has evident seasonal variations.

(2) There exist some temporary rivers in the plain due to seasonal changes of the Yellow River and the concentrated precipitations in summer, so that the soil humidity and water area have seasonal variations [32].

(3) Vertical soil humidity changes seasonally. In the south center of the Hetao Plain, the soil is wet over subsoil and is dry over topsoil, but after the raining season it reverses immediately [33].

(4) The seasonal water migration is caused by frozen soils in winter [34].

3.3.3 *Zoige*

Located at the junction of northwestern Sichuan and southeastern Gansu, in the east of the Tibetan Plateau with an average altitude of 3500 m, and crossed by the big turn of the Yellow River, Zoige is a key import water catchment to the upper reaches of the Yellow River and is one of the three biggest wetlands with the largest area of peat bog in China, which has a strong function of climate adjustment and a crucial role in the ecosystem [35]. Zoige is an important habitat for rare birds on plateau and is one of the five major pastoral areas with vast nature grasslands. Researches and investigations demonstrate that the wetlands and grasslands are degraded, which attract the more attention of relevant departments [35–37]. The radar satellite altimeter technique is a potential method for understanding the climate and environment variations, the water transmission over land, and the vegetation cover conditions in Zoige using the backscatter coefficients.

As shown in Figure 8(b), ground tracks of T/P before and after shifting orbit both cross Zoige, so that the impact of

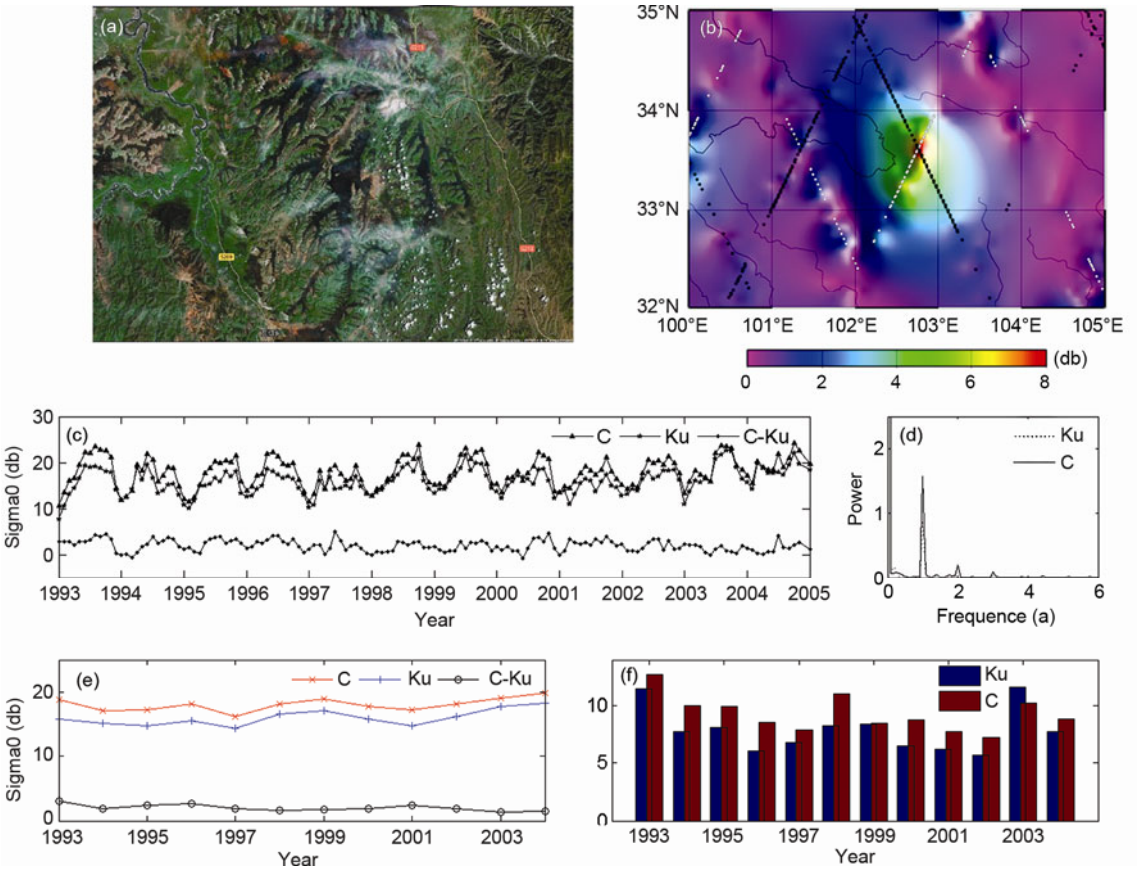

Figure 8 (a) The satellite image of Zoige; (b) the distribution of amplitudes at Ku band over Zoige and ground pass of T/P of which the white line is pre-orbit and the black is post-orbit; (c) the time series of monthly mean backscatters over Zoige; (d) the spectrum analysis for backscatters in Ku and C bands; (e) the yearly mean values at Ku and C bands as well as difference of two bands; (f) the maximum of annual variations each year for Ku and C bands.

shifting orbit to the observed data over Zoige is little. Figure 8(b) also shows that the amplitudes generally range from 4 to 8 db, and the maximum is 7.93 db. Figure 8(c) shows that the backscatter coefficients have evident signals of seasonal variations for two bands. The mean values of sigma0 are 16.84, 18.02, 1.54 db, respectively, for Ku band, C band, and their difference. The trends of three time series are consistent with each other, as the trough mainly presents at the end of winter or the beginning of spring and the crest mainly presents in summer. For the time series of sigma0 in Ku band, the annual and semi-annual amplitudes are 3.28 and 1.51 db, respectively. And the trend is 0.1211, an uptrend, probably due to the extended growing time of grasses because of the aggravation of climate warming, the decreasing of frozen soil over marsh, and increasing of grassland as the degrading of marsh. On the other hand, as the government pays more attention to the protection of wetlands and water storage, sand areas are turned into grasslands or irrigated grasslands [36]. Figure 8(e) shows that the absolute variations of sigma0 are high in years of 1993, 1998 and 2003, and low values are sequentially in 2000, 2001 and 2002, which may be connected with the precipitation of these years.

We can conclude that some reasons for high amplitudes of sigma0 in Zoige may lie in:

(1) The growth of vegetation over vast grasslands shows remarkable seasonal changes.

(2) Frozen soils, snow cover and the water freeze in winter contribute to the seasonal variations of land surface.

(3) Rainfalls are concentrated in summer and seasons of wet and dry are distinctly, causing some seasonal and temporal ponds, which contribute to evident seasonal variations of distribution and area of wetlands [34].

3.3.4 Sichuan Basin

The Sichuan Basin is one of four major basins in China, and several tributaries of the Yangtze River run through it. It is known as the land of abundance, for rich soils and advanced agriculture. For the time series shown in Figure 9(c), we can find that seasonal variations are evident for two bands over Sichuan Basin and the mean values of sigma0 are 24.51 and 22.51 db for C and Ku bands, respectively. In the time se-

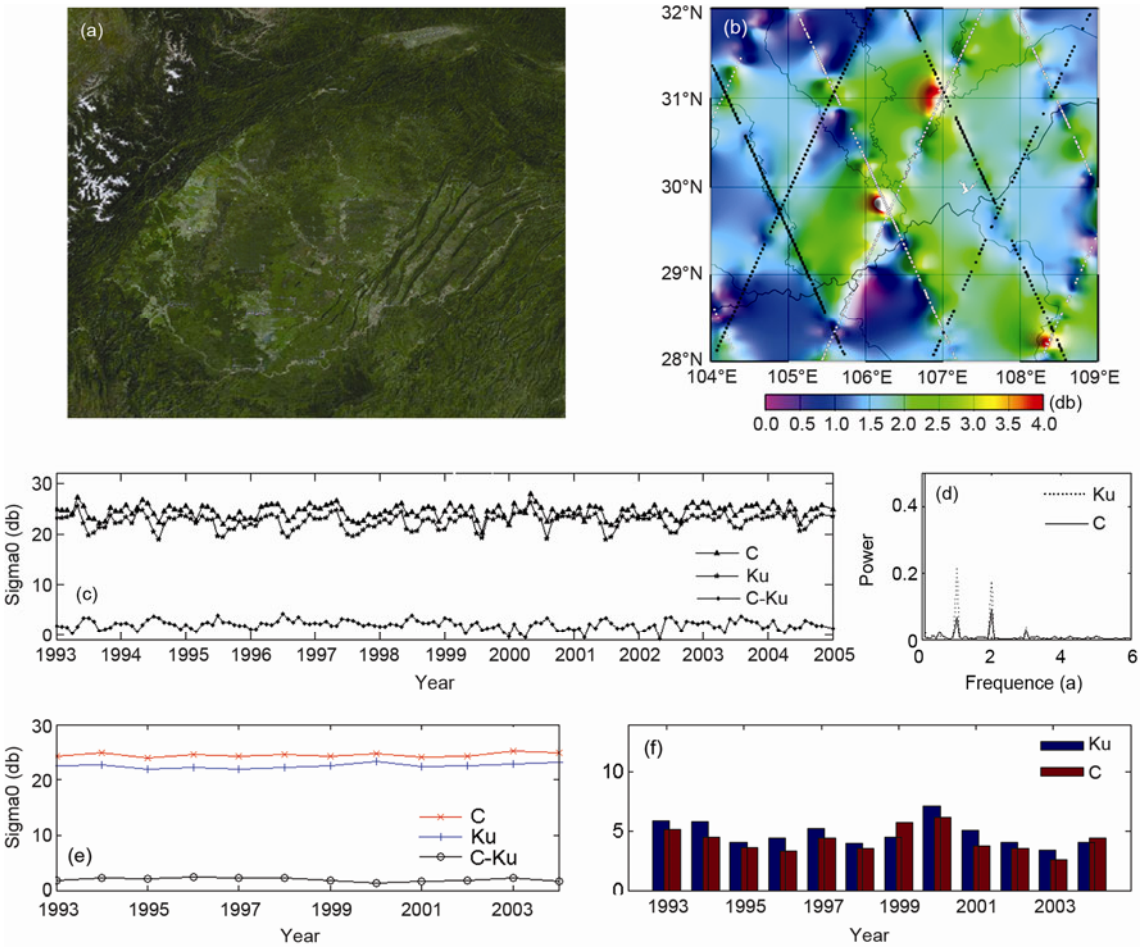

Figure 9 (a) The satellite image of Sichuan Basin; (b) amplitudes of semi-annual variations of simga0 at Ku band and ground pass of T/P of which the white line is pre-orbit and the black is post-orbit; (c) the time series of monthly mean backscatters over the Sichuan Basin; (d) the spectrum analysis for backscatters in Ku and C bands; (e) yearly mean values at Ku and C bands as well as difference values of two bands; (e) the maximum of annual variations each year for Ku and C bands over the Sichuan Basin.

ries there are three key points each year, of which the first peak is present in May, a trough appears in August, and an irregular fluctuation is in winter. The average difference value is 2.00 db with the maximum presenting in June each year regularly. Figure 9(e) shows that the yearly values of sigma0 are stable over 12 years, which is probably related to the regional climate conditions. The result of FFT analysis in Figure 9(d) shows that the powers of annual and semi-annual periods are nearly equivalent, which is significantly different from that over North China. And the amplitudes of the monthly time series shown in Figure 9(c) are 1.24 and 1.10 db, respectively, for annual and semi-annual variations at Ku band by the least squares method.

The seasonal variations of backscatter coefficients in Sichuan Basin have the special performance of peaks and troughs in the time series at two bands when compared to these in North China. This may be related to the growth of local crops, not consistent with that in North China, and then the temporal variations of rainfall.

3.3.5 *Taklimakan Desert*

The Taklimakan Desert is the largest desert in China and the second largest in the world, located in the center of the Tarim Basin in Xinjiang. The Taklimakan Desert is a better natural site for the calibration and validation of altimetry data for steady performance of sigma0 and other observations [19].

In order to eliminate the effect of the Hotan River and the Tarim River, we select the study area as (38°–40.5°N, 81.5°–87°E). Shown in Figure 10, the characteristics of sigma0 over the Taklimakan Desert are as follows:

(1) Compared with other land types, the sigm0 in the desert is steady with the low amplitude of seasonal variations, and Figure 10(e) shows that the absolute variations for two bands are mainly less than 2 db.

(2) Backscatter coefficients are more stable at Ku band than at C band as shown in Figure 10(c). There exist one crest each year and slight seasonal variations with an annual amplitude of 0.22 db for C band in the least squares sense. The reason may be that under the desert somewhere flows a continuous underground river to the Lop Nor; meanwhile, the capacity of penetration for microwave at C band is higher and the microwave at C band is more sensitive to water than that for Ku band.

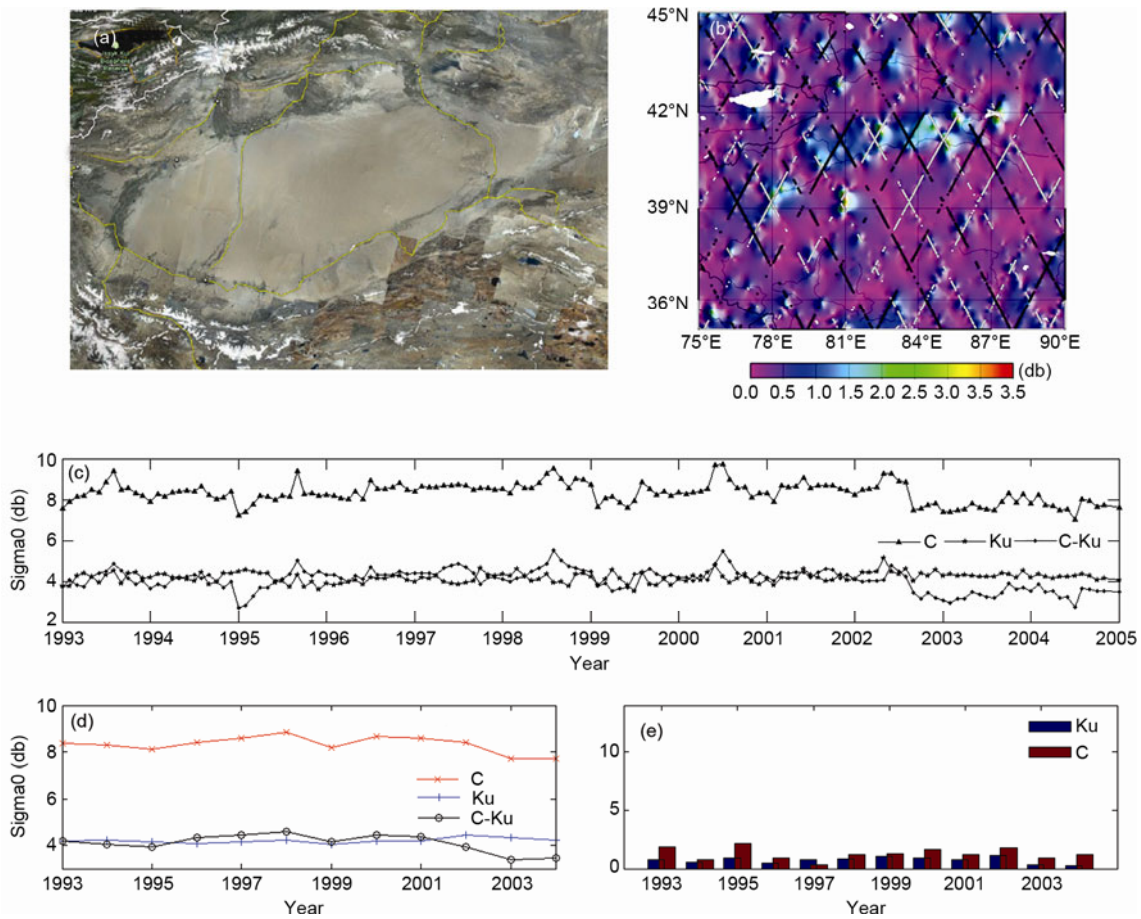

Figure 10 (a) Satellite image of Tarim Basin; (b) the distribution of amplitudes at Ku band over Taklimakan Desert and ground passes of T/P, of which the white line is pre-orbit and the black is post-orbit; (c) the time series of monthly mean backscatters over the Taklimakan Desert; (d) the yearly mean values at Ku and C bands as well as difference values of two bands; (e) the maximum values of annual variations each year for Ku and C bands over the Taklimakan Desert.

(3) The differences of sigma0s for both two bands are high. Averages for C, Ku bands, and their difference are 8.32, 4.21, and 4.11 db, respectively. And the maximum of the difference of two bands reaches up to 5.55 db, which indicates that values of backscatter coefficients at C band are double that at Ku band. This high value of difference is caused by different capacities of penetration over desert for different frequencies.

(4) After shifting orbit of T/P, backscatter coefficients for two bands are also steadier. Particularly for Ku band there presents more significantly backscattering characteristics of deserts, probably due to the passing of small inland rivers or large oasis for ground tracks of T/P before shifting orbit.

4 Correlation analysis with terrain slope

In order to study the influence of terrain slope, considered as the large scale topography, to backscatter coefficients of land surface, we use the slope data derived from 3″×3″ SRTM (shuttle radar topography mission with the resolution of 3 arcseconds) to do the correlation analysis with mean backscatter coefficients of sequential data in 12 years.

As an international project spearheaded by the National Geospatial-Intelligence Agency (NGA) and NASA, USA, the shuttle radar topography mission collected elevation data on a near-global scale to generate the most complete high-resolution digital topographic database over the Earth surface using a specially modified radar system that flew onboard the Space Shuttle Endeavour during an 11-day mission in February, 2000 (http://www2.jpl.nasa.gov/srtm/). The mission carried dual radar antennas of X band and C band, and products of two resolutions were achieved, that is, SRTM3 for 3″×3″ and SRTM1 for 1″×1″. And the SRTM3 of global data had been released to public in early 2004, but the SRTM1 over most areas has not been released, except only in the USA [38]. In this section, we use the slope data sets with a resolution of 90 m, provided by International Scientific Data Service Platform, Computer Network Information Center, Chinese Academy of Sciences (http://datamirror.csdb.cn). These data sets are derived from SRTM3 in China, processed by the 'Slope' function in 'Spatial Analysis' module of Arcgis 9.2, and covered the whole China.

Because the resolution of the used slope data sets is 3″×3″, which is different with the 5′×5′ grid data of backscatter coefficients, it is necessary to resample 3″×3″ slope data to 5′×5′. A lot of factors contribute to backscatter coefficient over lands, among which the topographic factor is just one. China is a large country with multiple types of land coverages and soils. So in order to minimize impacts of other factors to sigma0 and highlight the topography factor, we divide the study area into several small sub-areas to do correlation analysis separately, and the correlation coefficients are listed in Table 2.

As listed in Table 2, all correlation coefficients are negative, which indicates that the backscatter coefficients and the slope have a negative correlation. The strongest correlation appears in Liaoning and Jilin with a coefficient of –0.56, and the weakest correlation appears in the Taklimakan Desert as –0.11. And the average correlation coefficient is –0.35. The negative correlation indicates that backscatter coefficients have a decreasing trend as the slope increases, which matches the performance of backscatter coefficients over China land, that is, high values in flat areas and low in mountains. Given the way of working of altimeters and the physical process of backscattering, it can also infer the negative correlation of the backscatter and the slope. For the flat land surface, the backscattering component of scattering is high. In contrast, for fluctuated areas,

Table 2 Results of correlation analysis of sigma0 and slope

Area	Correlation coefficient
Tibetan Plateau (30°–35°N, 85–90°E)	–0.20
north Xinjiang & west Inner Mongolia (41°–50°N, 80°–95°E)	–0.23
Qinghai & east Tibet & west Sichuan (30°–35°N, 95°–100°E)	–0.43
Taklimakan Desert (37°–40°N, 80°–85°E)	–0.11
Tianshan Mountains & Junggar Basin (41°–45°N, 81°–90°E)	–0.41
Sichuan (26°–34°N, 97°–108°E)	–0.36
Yunnan & south Sichuan (23°–30°N, 98°–105°E)	–0.41
Guizhou (25°–30°N, 105°–110°E)	–0.30
Guangdong & Guangxi (22°–26°N, 106°–115°E)	–0.34
Shanxi (35°–40°N, 110°–115°E)	–0.36
West Shandong (35°–37°N, 115°–119°E)	–0.43
Heilongjiang & north Inner Mongolia (45°–54°N, 120°–130°E)	–0.46
Liaoning & Jilin (40°–45°N, 120°–130°E)	–0.56
Ningxia & north Shaanxi (35°–40°N, 105°–110°E)	–0.34
Mean	–0.35
Maximum	–0.56
Minimum	–0.11

the backscattering component is low and the diffuse reflection component is strong, so that the reception of backscatter power by the satellite altimeter is low, and so is the backscatter coefficient.

5 Conclusions

The temporal-spatial distributions of backscatter coefficients over lands in China detected by T/P mission are presented in the paper. The backscatter coefficients as measurements of T/P altimeter have close relationships with the property of land surface. Using continuous observations of T/P, we discuss the spatial distribution of sigma0 over China and nearby areas for Ku, C bands and their difference. Time series of sigma0 are analyzed and the amplitudes of seasonal variations are calculated. The temporal distribution of backscatter coefficients is also shown and studied. Based on natural characteristics of China land and the temporal-spatial distributions of backscatter coefficients, five sites, i.e. the Northeast Plain, the Hetao Plain, the Zoige wetlands, the Sichuan Basin, and the Taklimakan Desert, are selected to show the capacity of altimeter in detecting large typical areas and the potential ability to detect natural disasters and climate variations over land areas. The spatial correlation of sigma0 and topography is analyzed using slope data derived from SRTM3 and mean backscatter coefficients of sequential T/P data in 12 years, which quantifies the impact of topography factor to backscatter coefficients by correlation coefficients.

So far, about 30 years altimeter data in multiple bands can be achieved, mainly including Geosat, ERS-1/2, T/P, GFO, Jason-1/2, Envisat, and Cryosat-2. HY-2 as the first altimeter satellite of China was launched in 2008, which will further promote the satellite altimetric study and applications in China [39]. Because differences in satellite orbits and frequencies of radar pulse, the temporal and spatial resolutions are not the same, so it is a potential work to merge multiple altimeter data to improve the temporal and spatial resolutions. Moreover, the continuous data are useful for studying the long term variations of climate and environment on a global or regional scale. Future synergy with other space-bone sensors such as the active microwave wind scatterometers and MODIS at visible frequency is a very promising direction. In addition, to develop the backscatter model, which quantifies the water content of land and property of vegetation, needs further researches.

We are very grateful to the anonymous reviewers for their helpful suggestions and proposals. We thank AVISO for providing TOPEX/Poseidon GDR data. This work was supported by National Natural Science Foundation of China (Grant Nos. 40974004 and 40774009), International Sci & Tech Cooperation Program of China (Grant No. 2009DFB00130), Key Laboratory of Mapping from Space of NASMG, China (Grant No. K201103), and the R&I Team Supporting Program and Graduate Sci. & Tech Innovation Fund of SDUST, China (Grant No. YCB110010).

1 Rapley C G. Satellite radar altimeters. In: Vaughan R A, ed. Microwave Remote Sensing for Oceanographic and Marine Weather-Forecase Models. Dordrecht: Kluwer Academic, 1990
2 Fu L L, Cazenave A. Satellite Altimetry and Earth Sciences. San Diego: Academic Press, 2001
3 Rosmorduc V, Benveniste J, Lauret O, et al. Radar Altimetry Tutorial. ESA & CNES, 2009
4 Arthern R J, Wingham D J, Ridout A L. Controls on ERS altimeter measurements over ice sheets: Footprint-scale topography, backscatter fuctuations, and the dependence of microwave penetration depth on satellite orientation. J Geophys Res, 2001, 106: 33471–33484
5 Berry P A M. Topography from land radar altimeter data: Possibilities and restrictions. Phys Chem Earth Part A-Solid Earth and Geod, 2000, 25: 81–88
6 Brenner A C, Bindschadler R A, Thomas R H, et al. Slope-induced errors in radar altimetry over continental ice sheets. J Geophys Res, 1983, 88: 1617–1623
7 Guo J Y, Gao Y G, Hwang C W, et al. A multi-subwaveform parametric retracker of the radar satellite altimetric waveform and recovery of gravity anomalies over coastal oceans. Sci China Earth Sci, 2010, 53: 610–616
8 Guo J, Chang X, Gao Y, et al. Lake level variations monitoring with satellite altimetry waveform retracking. IEEE J Select Topics Appl Earth Obs Remote Sensing, 2009, 2: 80–86
9 Guo J, Sun J, Chang X, et al. Correlation analysis of Nino3.4 SST and inland lake level variations monitored with satellite altimetry: Case studies of lakes Hongze, Khanka, La-ang, Ulungur, Issyk-kul and Baikal. Terr Atmos Ocean Sci, 2011, 22: 203–213
10 Hwang C, Peng M F, Ning J, et al. Lake level variations in China from TOPEX/Poseidon altimetry: Data quality assessment and links to precipitation and ENSO. Geophys J Int, 2005, 161: 1–11
11 Ridley J, Strawbridge F, Card R, et al. Radar backscatter characteristics of a desert surface. Remote Sens Environ, 1996, 57: 63–78
12 Papa F, Legrésy B, Rémy F. Use of the Topex/Poseidon dual-frequency radar altimeter over land surfaces. Remote Sens Environ, 2003, 87: 136–147
13 Lacroix P, Legresy B, Coleman R, et al. Dual-frequency altimeter signal from Envisat on the Amery ice-shelf. Remote Sens Environ, 2007, 109: 285–294
14 Jiang W P, Chu Y H, Li J C, et al. Water level variation of Qinghai Lake from altimetric data (in Chinese). Geom Inf Sci Wuhan Univ, 2008, 33: 64–67
15 Berry P A M, Smith R G, Freeman J A, et al. Towards a new global digital elevation model. In: Sideris M G, ed. Observing Our Changing Earth. Int Assoc Geod Symp, 2009, 133: 431–435
16 Lacroix P, Dechambre M, Legrésy B, et al. On the use of the dual-frequency ENVISAT altimeter to determine snowpack properties of the Antarctic ice sheet. Remote Sens Environ, 2008, 112: 1712–1929
17 Skolnik M I. Radar Handbook. 2nd ed. Boston: McGraw-Hill, 1990
18 Lacroix P, Legresy B, Dechambre M, et al. Effects of snow properties on the dual frequency radar altimeter signal of Envisat over the antarctic ice-sheet. Proc Envisat Symp 2007, Montreux, Switzerland, 23–27 April, 2007, ESA SP-636
19 Berry P A M, Pinnock R A, Wilson H K. Land calibration and monitoring of ENVISAT RA-2 sigma0. Proce ERS-ENVISAT Symp, Gothenburg, Sweden, 2000. CD-Rom SP-461
20 Bramer S M C, Berry P A M, Johnson C P D. Analysis of ENVISAT RA-2 backscatter over natural land calibration targets. Proc 2004 Envisat ERS Symp (ESA SP-572). Salzburg, Austria, CD-Rom. #69, 16–10 September, 2004
21 Guo H D, Wang C, Wang X Y, et al. ERS-1 WSC data for global land surface monitoring (in Chinese). J Remote Sensing, 1997, 1: 277–281
22 Legresy B, Papa F, Remy F, et al. ENVISAT radar altimeter measurements over continental surfaces and ice caps using the ICE-2 retracking algorithm. Remote Sens Environ, 2005, 95: 150–163
23 Yang L, Du H, Ma H, et al. Use of the merged dual-frequency radar altimeter backscatter data over China land surface. IGARSS2010,

25–30 July, 2010. 1454–1457
24 Berry P A M, Bracke H, Jasper A. Retracking ERS-1 altimeter waveforms over land for topographic height determination:an expert systems approach. Proc. 3rd ERS Symp, Space at the Service of our Environment, Florence, Italy, March 1997. ESA SP-414
25 Guo J Y, Han Y B, Hwang C W. Analysis on motion of earth's center of mass observed with CHAMP mission. Sci China Ser G-Phys Mech Astron, 2008, 51: 1597–1606
26 Dunbar B, Hardin M. Mission to planet earth: TOPEX/Poseidon. NASA/CNES, 1992
27 Picot N, Case K, Desai S, et al. AVISO and PODAAC User Handbook: IGDR and GDR Jason Products. SMM-MU-M5-OP-13184-CN (AVISO), JPL D-21352 (PODAAC), 2003
28 Chen J Y, Li J C, Chao D B. Determination of the sea level height and sea surface topography in the China sea and neighbor by T/P altimeter data (in Chinese). J Wuhan Tech Univ Sur Map, 1995, 20: 322–326
29 Chu Y H, Li J C, Jin T Y, et al. Application of T/P altimeter backscatter data to land surface observation (in Chinese). J Geod Geodyn, 2009, 29: 104–108
30 Smith W H F, Wessel P. Gridding with continuous curvature splines in tension. Geophysics, 1990, 55: 293–305
31 Fang Y, Jiang T. Research on gridding of satellite altimetry data (in Chinese). Hydrogr Sur Map, 2010, 30: 30–33
32 Zhang W. Study on the temporal and spatial inversion of evapotranslation over Hetao Plain (in Chinese). Master's Dissertation. Beijing: Chinese Academy of Geological Science, 2008
33 Li R C. Analysis of variability of soil moisture over Hetao regions and its effect on short-term climate (in Chinese). Master's Dissertation. Lanzhou: Lanzhou University, 2006
34 Zhou D Y. Study of water immigration of seasonal merzlota over Hetao irrigated area (in Chinese). Inner Mongolia Water Resour, 1994, (1): 27–30
35 Xu H X, He Z W, Dan S M, et al. The wetlands in Zoige Plateau derived from quantitative remote sensing based on EOS/MODIS (in Chinese). J Glaciol Geocryl, 2007, 29: 450–455
36 Tang Y F. Studies on changes of surface water storage in Zoige Plateau (in Chinese). Master's Dissertation. Chengdu: Sichuan Agricultural University, 2009
37 Zhao K Y, He C Q. Influence of human activities on the mire in Zoige Plateau and counter measure (in Chinese). Sci Geogr Sin, 2000, 20: 444–449
38 Chen J Y. Quality evaluation of topographic data from SRTM3 and GTOPO30 (in Chinese). Geom Inf Sci Wuhan Univ, 2005, 30: 941–944
39 Guo J Y, Qin J, Kong Q L, et al. On simulation of precise orbit determination of HY-2 with centimeter precision based on satellite-borne GPS technique. Appl Geophys, 2012, 9: 95–107